Screening and Compounding of Gas Hydrate Anti-agglomerants from Commercial Additives through Morphology Observation

ARTICLE *in* ENERGY & FUELS · APRIL 2013

Impact Factor: 2.79 · DOI: 10.1021/ef400147j

9 AUTHORS, INCLUDING:

Jun Chen
South China University of Technology
21 PUBLICATIONS **134** CITATIONS
SEE PROFILE

Chang-Yu Sun
China University of Petroleum
108 PUBLICATIONS **1,293** CITATIONS
SEE PROFILE

Bei Liu
China University of Petroleum
73 PUBLICATIONS **983** CITATIONS
SEE PROFILE

energy&fuels

Article

pubs.acs.org/EF

Screening and Compounding of Gas Hydrate Anti-agglomerants from Commercial Additives through Morphology Observation

Jun Chen, Chang-Yu Sun,* Bao-Zi Peng, Bei Liu, Si Si, Meng-Lei Jia, Liang Mu, Ke-Le Yan, and Guang-Jin Chen*

State Key Laboratory of Heavy Oil Processing, China University of Petroleum, Beijing 102249, People's Republic of China

ABSTRACT: The anti-agglomeration performance of single or compounded commercial chemical additives with/without the addition of alcohol as a co-surfactant was evaluated using a sapphire cell and an autoclave reactor with a focused beam reflectance measurement (FBRM) probe. Five kinds of gas hydrate morphologies, clumpy-like, slush-like, flocculent-like, slurry-like, and powder-like, were found during evaluating the effect of the commercial additives in (water + oil) systems. The experimental results showed that AEO-3 combined with some commercial chemical additives, especially Span 20, exhibits good anti-agglomeration performance. The hydrate slurry thus formed has a high stability and will not result in agglomeration for a long period of time. A compounded inhibition mechanism, in which one of the components disperses water droplet in the oil phase and the other component prevents formed hydrate from agglomeration, was proposed. A new structure of hydrate anti-agglomerant was designed according to the evaluating results of the single or compounded commercial additives with/without the addition of alcohol material.

1. INTRODUCTION

Hydrate formation has been well-known as one of the reasons that can cause pipeline blockages.[1] It is still one of the important concerned issues in deepwater field developments. Although there exists a promising method for dissociating hydrate to solve hydrate blockages in oil and gas pipelines,[2] adding thermodynamic or low-dosage hydrate inhibitors to prevent the hydrate plug is the most favorite choice. Traditional thermodynamic hydrate inhibitors, such as methanol, glycol, and saline solution, were usually added to let the production line out of the gas hydrate formation region.[3−7] However, the amount of thermodynamic inhibitors often reaches 20−50 wt % or more, which is quite uneconomic, while some thermodynamic inhibitors, such as methanol, are environmentally unfriendly.[8] Low-dosage hydrate inhibitors, including kinetic inhibitors (KIs) and anti-agglomerants (AAs), have attracted much attention in recent years because of their low dosage and economy.[9−11] KIs chiefly inhibit hydrate formation for a long period of time by extending the induction time for hydrate nucleation, while AAs prevent the plugging of pipelines by inhibiting the agglomeration of hydrate particles. In comparison, for the fluid-containing hydrocarbon phase, AAs enable the hydrates to form as transportable low-viscous fluid-containing hydrate particles and cannot be limited by the subcooling. This kind of hydrate-containing fluid might become an alternative approach for oil and gas transportation because a large amount of natural gas can be stored in the form of hydrate. In addition, some technological applications based on hydrates, such as separation of gas mixtures via forming hydrate,[12] also need a high performance of AAs to ensure the flow of the hydrate-containing fluid.

Many AAs, including water-in-oil emulsifying AAs and "hydrate-philic" AAs,[9,13−15] were reported recently. Most used methods to develop AAs are screening commercial surfactants, synthesizing new types of inhibitor, or extracting some of the components from special nature materials.[15−18] The evaluations of AAs are usually performed using rocking cells. Maccioni and Passucci[19] studied two categories of AAs, quaternary ammonium salts and quaternary phosphonium salts. They found that short alkyl chains have a better anti-agglomeration effect than those with long chains in phosphonium salts for a water/gas system. Huo et al.[15] have tested commercially available surfactants as AAs and found that Span 20 performed well as an AA. In addition, some loop experimental apparatuses were also used to test the performance of low-dosage hydrate inhibitors.[20−22]

Morphology and particle size magnitude are two important factors for characterizing the effect of AAs. It is more direct and quantitative to develop AAs from visual observation and *in situ* online measurement of size distribution before/after hydrate formation. In this work, some kinds of single or compounded commercial chemical additives were evaluated to examine their ability of preventing gas hydrate from agglomeration through visual observation method in a sapphire cell, which has been used to assess the effect of hydrate KIs in our previous work.[23] The chord length distribution of water droplet/hydrate particle was also measured for typical (water + diesel oil + commercial surfactant) systems. The morphology of hydrate-containing fluid and the effect of the commercial chemical additives were discussed. A compounded inhibiting mechanism was proposed to prevent hydrate from agglomeration, and a new structure of AA was designed.

2. EXPERIMENTAL SECTION

2.1. Materials. To evaluate the performance of the AAs, twice distilled water with/without sodium chloride and diesel oil were mixed

Received: January 25, 2013
Revised: March 26, 2013
Published: April 17, 2013

   dx.doi.org/10.1021/ef400147j | *Energy Fuels* 2013, 27, 2488−2496

to make up the liquid phase. The composition of the diesel oil was shown in Table 1. The hydrophilic and lipophilic commercial

Table 1. Composition of the Diesel Oil Used for Evaluating the Performance of AAs

component		mol %	wt %
C_7	heptanes	0.22	0.10
C_8	octanes	1.35	0.70
C_9	nonanes	3.60	2.09
C_{10}	decanes	3.70	2.39
C_{11}	undecanes	5.90	4.19
C_{12}	dodecanes	5.16	3.99
C_{13}	tridecanes	8.34	6.98
C_{14}	tetradecanes	13.61	12.26
C_{15}	pentadecanes	11.37	10.97
C_{16}	hexadecanes	10.08	10.37
C_{17}	heptadecanes	9.59	10.47
C_{18}	octadecanes	8.71	10.07
C_{20}	eicosanes	11.42	14.66
C_{24}	tetracosanes	6.81	10.47
C_{28+}	octacosanes plus	0.15	0.30
	total	100.00	100.00

surfactants, analytically pure, with the hydrophilic−lipophilic balance (HLB) values ranging from 1.8 to 16.7 and purchased from Beijing Chemical Reagents Company (BCRC), China, were added to form water in a diesel oil dispersed system. Other analytical reagents, such as tetrabutylammonium bromide (TBAB), ethylene glycol (EG), glycerol, and polyethylene glycol (PEG), were also purchased from BCRC. The commercial and chemical names of the additives and part of HLB values used in this work were listed in Table 2. The dosage of

Table 2. Additives Used in the Evaluation Experiments

number	commercial name	chemical name	HLB
1	Span 20	sorbitan monolaurate	8.6
2	Span 85	sorbitan trioleate	1.8
3	Tween 20	polyoxyethylene sorbitan monolaurate	16.7
4	Tween 60	polyoxyethylene sorbitan monostearate	14.9
5	Tween 80	polyoxyethylene sorbitan monooleate	15.0
6	AEO-3	fatty alcohol polyoxyethylene ether $N = 3$	6−7
7	AEO-5	fatty alcohol polyoxyethylene ether $N = 5$	10−11
8	Triton X-100	octylphenylpolyethylene glycol ether	
9	OE 6	polyethylene glycol monolaurate	10
10	TX-7	heptyl phenol polyethylene glycol ether	10−11
11	SA-40	dodecyl dimethyl betaine	
12	EL-40	polyoxyethylene castor oil	13−14
13	TBAB	tetrabutylammonium bromide	
14	EG	ethylene glycol	
15	glycerol	glycerol	
16	PEG	polyethylene glycol	

the surfactants and other additives was described as the percentage of them relative to the quantity of water. To simulate the hydrate formation in the oil and gas transportation pipeline, natural gas in a real operating environment was adopted to form hydrate, whose composition was listed in Table 3.

2.2. Apparatus and Procedures. The schematic diagram of the experimental apparatus used in this work for estimating the

Table 3. Composition of Natural Gas Used To Form Hydrate

component	mol %
methane	85.67
ethane	2.58
propane	1.21
isobutane	0.21
n-butane	0.20
isopentane	0.05
n-pentane	0.02
hexane	0.04
nitrogen	1.73
carbon dioxide	8.29

performance of the commercial additives as AAs was shown in Figure 1. It mainly contains a sapphire cell and an air bath. The detailed

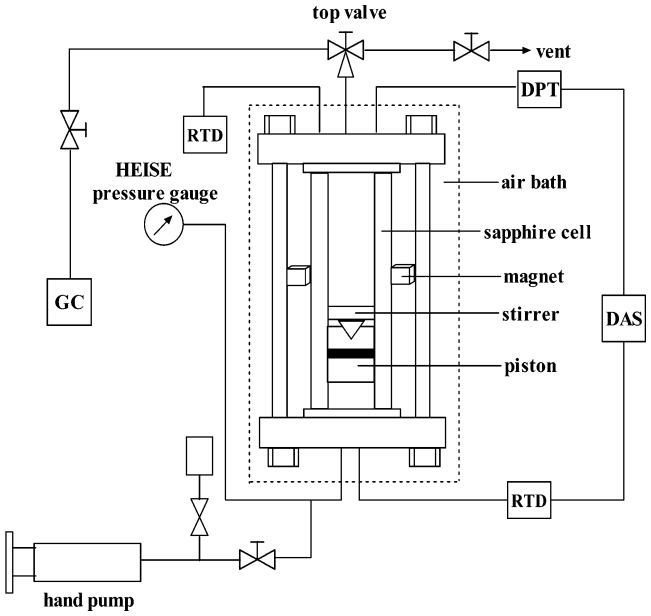

Figure 1. Schematic diagram of the experimental apparatus. RTD, resistance thermocouple detector; DPT, differential pressure transducer; GC, gas cylinder; and DAS, data acquisition system.

descriptions of this apparatus can be referred to our previous works.[24−26] Chen et al.[23] have used this apparatus to assess the onset time of hydrate formation by adding different hydrate KIs, Inhibex 301, Inhibex 501, and VC-713, through visual observation method.

The main experimental procedures are given as follows. First, the sapphire cell was washed 3 times with twice-distilled water to remove the possible residual impurities and then dried by nitrogen purging. After preparing the water and diesel oil at a specified oil/water ratio, the desired quantities of water + diesel oil plus a certain amount of one commercial additive or compounded additives were charged into the sapphire cell. Subsequently, the cell was installed onto the apparatus, and the stirrer was started to ensure that water was dispersed in the oil phase. At the same time, the temperature of the air bath was set to the experimental value and maintained constant. In general, it took more than 5 h to achieve thermal equilibrium in the air bath, sapphire cell, and (water + diesel oil) dispersed system in the cell. Thereafter, the cell and fluid pipelines were evacuated, and natural gas was charged into the cell to induce a large ratio of water be turned into hydrate. To eliminate the influence of the change of gas phase composition resulting from the dissolution of natural gas in the (water + diesel oil) dispersed system and hydrate formation, the gas in the cell was

dx.doi.org/10.1021/ef400147j | Energy Fuels 2013, 27, 2488−2496

replaced with a natural gas sample in the gas cylinder several times during the experiment, while the pressure was maintained constant. Afterward, the inlet valve was closed, and the stirrer was maintained at a speed of 120 rpm. Morphology of fluid during/after the hydrate formation process was observed and recorded.

Other groups of experiments with different additives or oil/water ratios will be proceeded according to the above procedures. Considering that alcohols can be used as co-surfactants to help hydrate anti-agglomeration, three kinds of alcohols were added in some systems when evaluating the performance of compounded surfactants.[27]

For some kinds of samples, a typical chord length distribution of the (water + diesel oil) dispersed system before/after hydrate formation was also analyzed in an autoclave reactor with a focused beam reflectance measurement (FBRM) D600X probe, purchased from Mettler-Toledo Lasentec. Figure 2 shows a schematic diagram of the

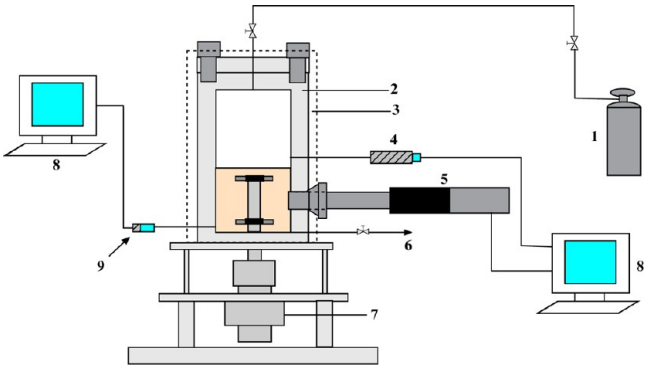

Figure 2. Schematic diagram of the experimental apparatus for measuring water droplet/hydrate particle distribution in the (water + diesel oil) dispersed system: 1, gas cylinder; 2, autoclave reactor; 3, water bath; 4, pressure transducer; 5, FBRM probe; 6, vent; 7, magnetic stirrer; 8, computer; and 9, thermocouple.

experimental apparatus used for measuring water droplet/hydrate particle chord length distribution in the (water + diesel oil) dispersed system. The apparatus is mainly constituted by three parts: a high-pressure autoclave with a water bath and magnetic stirrer, FBRM probe, and data collection system. The effective internal volume of the reactor is 535 mL (51.84 mm in diameter and 320 mm in depth). The schematic diagram of the FBRM probe is shown in Figure 3. There is a rotating optical lens at the probe tip, which can deflect the laser, as shown in Figure 3a. The emitted laser is reflected if it scans across the surface of a particle, as shown in Figure 3b. The chord length can then be determined by the product of the measurement reflectance time and the laser scan speed. The FBRM probe has been used to measure the water droplet or hydrate particle size in the oil phase in recent years.[28−30] More information on the probe and technique is referenced in the user's manual.[31] The following procedure is used to measure the chord length distribution of the (water + diesel oil) dispersed system.

The reactor and all of the connections were flushed with hot distilled water, dried with pure nitrogen, and evacuated. The FBRM probe was cleaned to reach the measured acquirement, in which the total count of particles was less than 150 before measurement. Subsequently, 220 mL of prepared (water + diesel oil) dispersed fluid with a certain amount of additive was injected into the reactor, and it was evacuated again to remove the air dissolved in the solution. The temperature of the water bath was specified at 274.2 K, and the stirrer was started to ensure that the water droplet homogeneously dispersed in the diesel oil phase. When the temperature was stable and maintained constant for about 4 h, natural gas was injected into the reactor to make sure that most of the water converted into hydrate, while the subcooling was about 10 K. Chord length distributions of the water droplet/hydrate particle in the (water + diesel oil) dispersed system before hydrate formation, after most hydrate formation, and after 10 h of stopping mixing were measured.

3. RESULTS AND DISCUSSION

3.1. Morphology of Formed Gas Hydrate. During the evaluation experiments on the effect of the commercial additives, five kinds of gas hydrate morphologies formed from (water + diesel oil) systems were found, that is, gas hydrates in clumpy-like, slush-like, flocculent-like, slurry-like, and powder-like morphologies. The typical pictures are shown in Figure 4. Clumpy-like hydrate is that the formed hydrate deposits at the bottom of the cell and sticks to the cell wall, meaning that the commercial additive becomes invalid in (water + oil) systems. Slush-like hydrate is relatively infrequently found during the evaluation of the commercial additives in this work, which can stick to the cell wall with a viscous force. Flocculent-like hydrate is fluffy-like cotton morphology and can be dispersed in the diesel oil phase. Slurry-like hydrate is that the formed hydrate homogeneously dispersed in the diesel oil phase in slurry shape with a certain flow ability. Powder-like hydrate is that hydrate is dispersed in the diesel oil phase in the form of particles with a certain flow ability. Different morphologies are also found in previous loop studies in SINTEF.[9]

Although fluids containing slush-like or flocculent-like hydrate can flow under some circumstances, they tend to turn into clumpy-like hydrate in general. Figure 5 shows the variation process of the morphology of hydrate formed from the (5 vol % water + 95 vol % diesel oil + additive) dispersed system with a salinity of 3 wt %. The compounded additives are (3 wt % AEO-3 + 3 wt % TBAB + 2 wt % EG) based on water. It can be found that, at first, the water drop was dispersed in the diesel oil system before the formation of hydrate, as shown in Figure 5a. With the continuous formation of hydrate, it changes

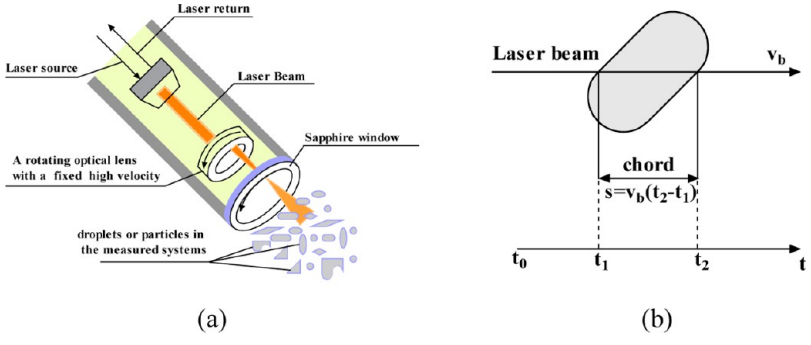

Figure 3. Schematic diagram for measuring the chord length distribution by the focused beam reflectance method: (a) FBRM probe and (b) measurement of a particle chord length.

dx.doi.org/10.1021/ef400147j | Energy Fuels 2013, 27, 2488−2496

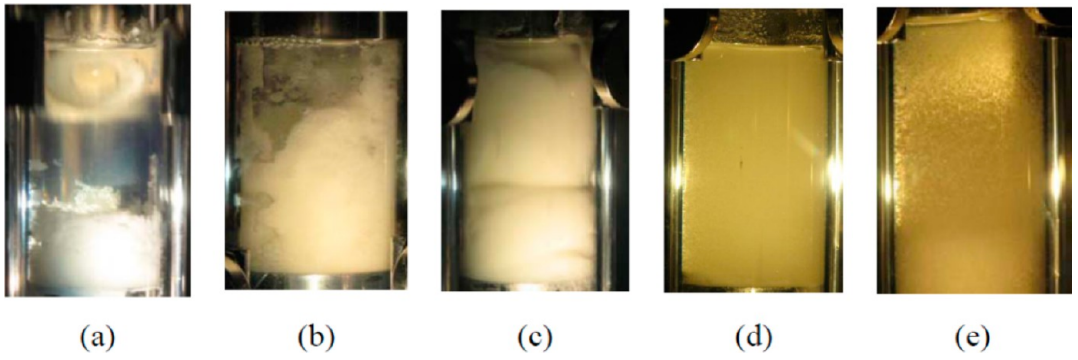

Figure 4. Morphology of the hydrate formed from (water + diesel oil) systems with the commercial additives: (a) clumpy-like, (b) slush-like, (c) flocculent-like, (d) slurry-like, and (e) powder-like. The inner diameter of the sapphire cell is 2.54 cm.

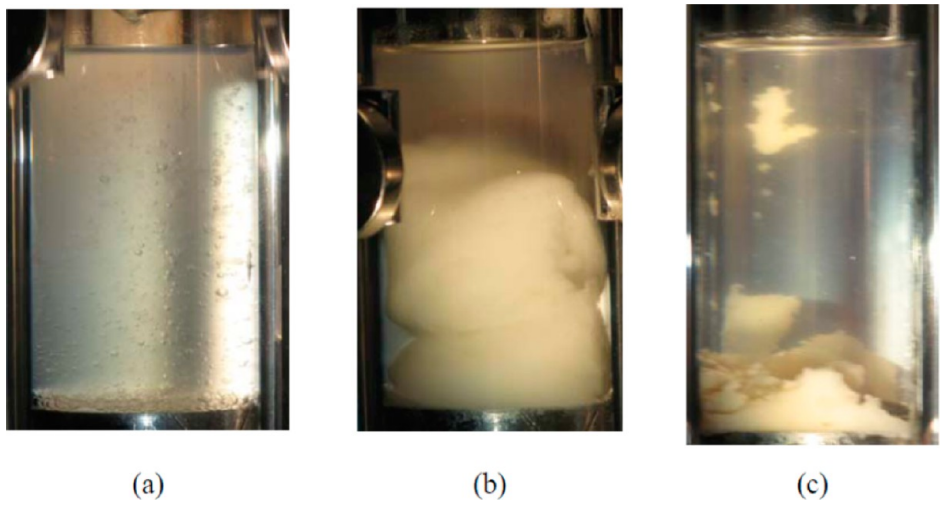

Figure 5. Morphology change of the (5 vol % water + 95 vol % diesel oil + 3 wt % AEO-3 + 3 wt % TBAB + 2 wt % EG) system with a salinity of 3 wt % during the hydrate formation process: (a) water in diesel oil dispersed systems, (b) flocculent-like hydrate, and (c) clumpy-like hydrate.

into flocculent-like hydrate (Figure 5b) and finally into clumpy-like hydrate (Figure 5c). In comparison to the photo of water in the diesel oil dispersed system (Figure 5a), it was interesting to find that the formed flocculent-like hydrate (Figure 5b) can expand and occupy a large part of the volume of the fluid, although the volume of water in the initial fluid is only 5%. Both slush-like and flocculent-like hydrates can be considered as "wet" hydrate in this work, in which water was partly transformed. In comparison to "wet" hydrate, clumpy-like, slurry-like, and powder-like hydrates can be considered as the "dry" hydrate. Most of the water transforms into hydrate in these three situations, and the formed hydrate can be dispersed in the oil phase when slurry-like and powder-like hydrates formed.

3.2. Performance of a Single Additive. The performance of a single additive was first experimentally evaluated. The water cut of the (water + diesel oil) system is 30 vol %, and the mass fraction of the additive is set at 3 wt %. The experimental temperature is 274.2 K. Other experimental conditions, such as the experimental pressure and subcooling, which is defined as the temperature difference between the equilibrium and experimental states, were listed in Table 4. The hydrate equilibrium conditions for evaluating the subcooling were calculated by the Chen−Guo hydrate model.[32] The morphology of hydrate formed under the corresponding experimental conditions was also listed in Table 4. From Table 4, it can be found that most of the additives can make the formed gas hydrate dispersed in the oil phase as a slurry-like morphology when the subcooling is about 10 K, except Tween 60 and Tx-7.

Table 4. Morphology for Hydrate Formed from the (30 vol % Water + 70 vol % Diesel Oil) System after Adding 3 wt % Single Additive

additive	subcooling (K)	P (MPa)	morphology
Tween 20	9.7	3.59	slurry-like
Tween 60	9.7	3.59	clumpy-like
Tween 80	9.6	3.50	slurry-like
Triton X-100	9.8	3.58	slurry-like
Span 20	9.6	3.54	slurry-like
Span 85	9.9	3.67	slurry-like
AEO-3	9.9	3.68	slurry-like
AEO-5	9.8	3.62	slurry-like
EL 40	9.7	3.58	slurry-like
OE 6	9.4	3.45	slurry-like
Tx-7	10.0	3.74	clumpy-like
SA-40	9.7	3.59	slurry-like

Although slurry-like hydrate formed for some single-additive systems when water cut is 30 vol % and the additive content is 3 wt %, hydrate in this state is usually very sticky and not suitable for the flow in the pipelines. A typical picture was shown in Figure 6a for (30 vol % water + 70 vol % diesel oil + 3 wt % AEO-3) under the subcooling of 9.9 K. Although hydrate particles do not agglomerate with each other, the formed

dx.doi.org/10.1021/ef400147j | Energy Fuels 2013, 27, 2488−2496

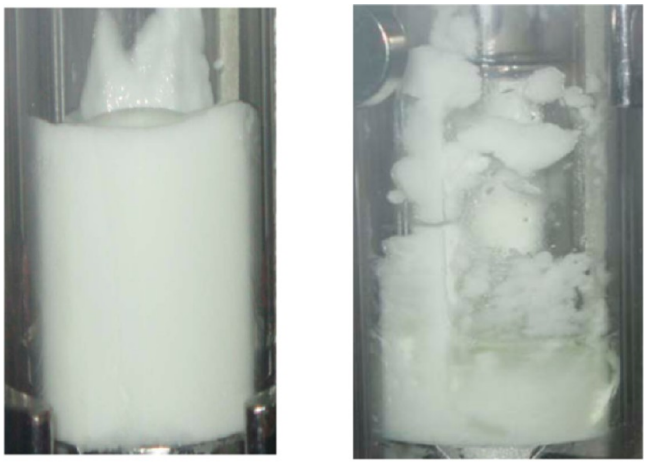

(a) (b)

Figure 6. Morphology of the formed hydrate: (a) (30 vol % water + 70 vol % diesel oil + 3 wt % AEO-3) system under the subcooling of 9.9 K and (b) (30 vol % water + 70 vol % diesel oil + 1 wt % AEO-3) system under the subcooling of 9.5 K.

hydrate slurry is very sticky. There is a metallic gasket in the sapphire cell, and it can be raised or released by the magnetic force produced from outside of the sapphire cell. The sticky aspect of the fluid could be roughly evaluated by the movement of the metallic gasket in the solution. For systems in which the content of a single additive is more than 3 wt %, a more sticky hydrate slurry was formed from the rough evaluation by the metallic gasket. It is known that the viscosity of the formed hydrate-containing fluid would play an important role during the oil and gas transportation via forming a hydrate slurry. A high apparent viscosity of the hydrate slurry is not in favor of its flow in the pipeline. If the dosage of single additives is decreased, the anti-agglomeration performance will decrease and hydrate will agglomerate at the bottom of the sapphire cell. Clumpy-like hydrate will form, as shown in Figure 6b, for the (30 vol % water + 70 vol % diesel oil + 1 wt % AEO-3) system under the subcooling of 9.5 K. Therefore, a single additive in general is not better used for AA when the water cut is high in the water-in-oil emulsion.

This phenomenon is also similar for the systems with low initial water cut in the emulsion. Figure 7 shows the morphology change for the (5 vol % water + 95 vol % diesel oil + 3 wt % AEO-3) system before and after the formation of hydrate under the subcooling of 9.6 K. It can be seen that, although AEO-3 cannot disperse water well in the diesel oil phase before hydrate formation, it can disperse the formed hydrate in the diesel oil phase well. However, the size of the formed hydrate particles is large. When the stirring is stopped, the hydrate particle will pile up on the bottom of the cell, although it can still disperse in the oil phase again when the stirring is started. The formed hydrate fluid is also relatively viscous because 3 wt % AEO-3 was added.

From Table 4, it can be found that slurry-like hydrate forms for the (30 vol % water + 70 vol % diesel oil) system containg 3 wt % Span 20. With the decrease of the water cut, it will change to powder-like hydrate. From the evaluation of Span 20 systemically,[22] it was found that Span 20 could disperse water well into the oil phase as the form of a droplet, forming emulsion of water-in-oil. The initially formed hydrate will be in the form of fine particles. However, it fails to disperse

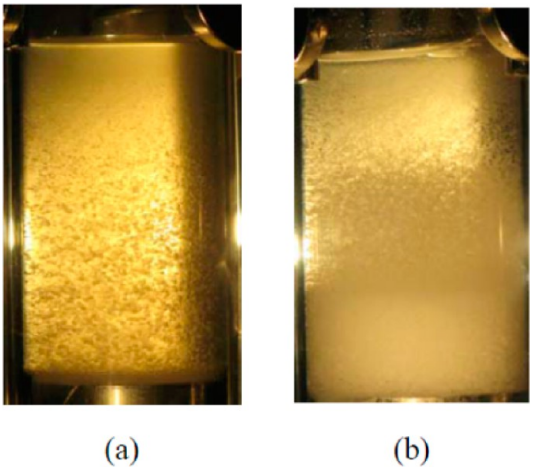

(a) (b)

Figure 7. Morphology change of the (5 vol % water + 95 vol % diesel oil + 3 wt % AEO-3) hydrate during the formation of hydrate with the subcooling of 9.6 K: (a) before hydrate formation and (b) after most of the water has converted into hydrate.

the hydrate particles with Span 20 alone at lower concentrations.

From the evaluation and analysis of a single-additive performance on (water + diesel oil) systems, it can be found that a single additive is usually not suitable for preventing hydrate from agglomerating, although some kinds of single additives can make the formed hydrate as a slurry-like or powder-like morphology. On the other hand, some single additives may possess a certain function; for example, AEO-3 may play a role to prevent formed hydrate from agglomeration, and Span 20 may play a role to disperse water into oil and make the initially formed hydrate in the form of fine particles. These performances of a single additive imply a potential possibility to prevent hydrate from agglomeration by adding compounded additives of these single additives.

3.3. Performance of Compounded Additives. During evaluation of the anti-agglomerating performance of a single additive, it was found that AEO-3 can disperse the formed hydrate in the diesel oil phase well, except that it cannot disperse water well in the diesel oil phase before hydrate formation. The compound additives of AEO-3 with other additives, particularly those possessing the performance of dispersing water into the oil phase, were then examined to investigate their anti-agglomeration effect. Some kinds of alcohols, such as EG, PEG, and glycerol, were added in some systems to act as an assistant when evaluating the performance of compounded surfactants. The water cut is specified at 5−30 vol %, with a salinity of 3 wt %. The evaluated results of compounded commercial additives were listed in Table 5, where the experimental conditions, such as oil and water cut, mass fraction and types of additives, temperature, pressure, and subcooling, were included. The whole dosage of compounded additives is from 3 to 8 wt % to examine the influence of additive dosage on the viscosity of the hydrate-containing systems.

From Table 5, it was found that most of the additives combined with AEO-3 showed the hydrate morphology of flocculent-like or slurry-like. Quaternary ammonium salts can be considered as AAs in the reported literature.[33] TBAB is a typical quaternary ammonium salt; however, hydrate formed from the (water + oil) system by adding the compounded additives containing (3 wt % AEO-3 + 3 wt % TBAB + 2 wt % EG)

dx.doi.org/10.1021/ef400147j | Energy Fuels 2013, 27, 2488−2496

Table 5. Compounded Additive Test Used as AAs

additives	mass (%)	diesel oil (vol %)	saline water (vol %)	T (K)	P (MPa)	subcooling (K)	morphology
2:1:5 AEO-3/ TritonX-100/EG	8	90	10	277.2	6.62	8.3	slush-like
2:1:3 AEO-3/Triton X-100/EG	6	90	10	277.2	6.19	8.0	flocculent-like
3:2 AEO-3/EG	5	90	10	277.2	6.46	8.8	flocculent-like
2:1:1 AEO-3/Triton X-100/EG	4	90	10	277.2	6.00	9.2	flocculent-like
2:1:2 AEO-3/Triton X-100/EG	5	90	10	277.2	6.59	9.1	flocculent-like
2:1:3 AEO-3/Triton X-100/EG	6	95	5	277.2	6.45	8.3	flocculent-like
3:2:2 AEO-3/Triton X-100/EG	7	95	5	277.2	6.15	8.7	flocculent-like
2:1:2 AEO-3/Triton X-100/PEG	5	95	5	276.2	5.98	9.5	clumpy-like
3:1:3 AEO-3/Triton X-100/EG	7	95	5	277.2	6.38	8.2	slurry-like
3:2:2 AEO-3/Triton X-100/EG	7	95	5	274.2	4.49	9.5	slurry-like
3:2:2 AEO-3/Triton X-100/EG	7	90	10	274.2	4.25	9.1	flocculent-like
3:2:2 AEO-3/Triton X-100/PEG	7	95	5	274.2	4.15	9.0	flocculent-like
3:2:2 AEO-3/EL 40/EG	7	95	5	274.2	4.10	8.9	clumpy-like
3:2:2 AEO-3/OE 6/EG	7	95	5	274.2	4.68	9.8	clumpy-like
1:1 AEO-3/Span 20	4	95	5	274.2	3.52	9.6	slurry-like
3:2 AEO-3/Span 20	5	70	30	274.2	3.25	9.1	slurry-like
3:2:2 AEO-3/Triton X-100/glycerol	7	95	5	274.2	3.98	8.5	flocculent-like
2:1 AEO-3/Span 20	3	95	5	274.2	3.44	9.5	powder-like
3:3:2 AEO-3/TBAB/EG	8	95	5	274.2	3.85	8.5	clumpy-like

shows clumpy-like morphology. AEO-3 combined with Span 20 shows good anti-agglomeration performance, in which the formed hydrate is slurry-like or powder-like. From a comparison of the mass fraction of additives and morphology of hydrate formed, as shown in Table 5, the better compounded additive is (2 wt % AEO-3 + 1 wt % Span 20) without the addition of alcohols. Figure 8 shows the morphology of gas hydrate formed with compounded additives of AEO-3 and Span 20. It can be found that the slurry-like or powder-like hydrate was formed for 30 or 5 vol % water cut with compounded additives of (3 wt % AEO-3 + 2 wt % Span 20) or (2 wt % AEO-3 + 1 wt % Span 20), respectively. The hydrates formed from (AEO-3 + Span 20) compounded additives possess the advantages of AEO-3 of dispersing the formed hydrate in the oil phase and Span 20 of dispersing water into oil. The formed hydrates are evenly dispersed in the diesel oil phase and do not agglomerate. In comparison to a single AEO-3 system, as shown in Figure 6, hydrate formed from the (5 vol % water + 95 vol % diesel oil) system by adding (AEO-3 + Span 20) compounded additives is a uniform powder-like morphology. It changes to slurry-like morphology when the water cut increases to 30% and the viscosity of the slurry-like hydrate-containing fluid is significantly low, as shown in Figure 8a, from the visual observation and the movement of the metallic gasket in the liquid phase. In addition, the stability of hydrate-containing fluid formed by adding (AEO-3 + Span 20) compounded additives is also high, and it can be maintained at the same morphology in a static condition for more than 10 h.

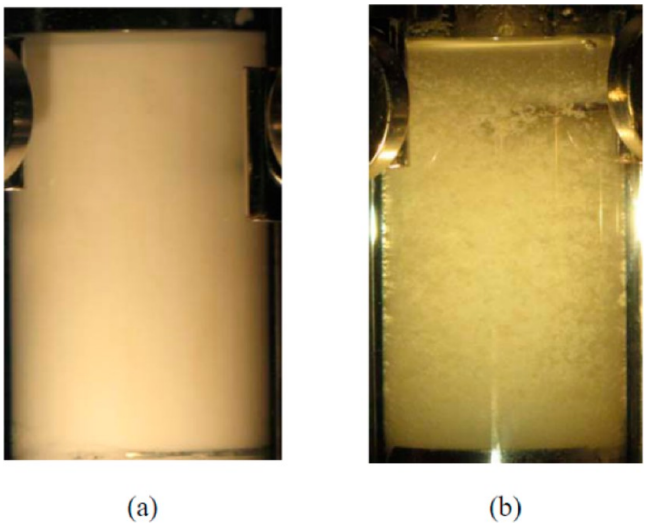

Figure 8. Morphology of natural gas hydrate in the presence of compounded additives: (a) (30 vol % water + 70 vol % diesel oil) system with (3 wt % AEO-3 + 2 wt % Span 20) and (b) (5 vol % water + 95 vol % diesel oil) system with (2 wt % AEO-3 + 1 wt % Span 20).

Chord length distribution of the water droplet/hydrate particle in the oil phase before and after the formation of hydrate was also investigated using the FBRM probe. A typical example was taken for the (methane + 5 vol % water + 95 vol % diesel oil) dispersed system with compounded additives (2 wt % AEO-3 + 1 wt % Span 20) at 274.2 K and 8.62 MPa. Figure 9 shows the change of the chord length distribution of the water droplet/hydrate particle in the oil phase at different time stages: (a) (water + diesel oil) emulsion, (b) most of the water droplets

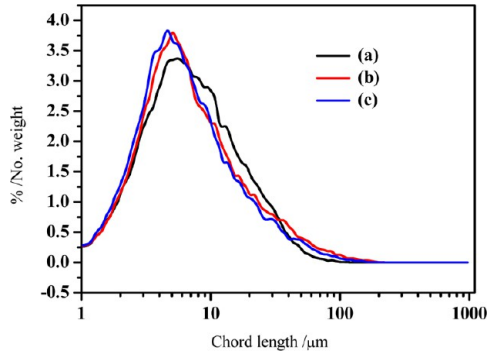

Figure 9. Chord length distribution of the water droplet/methane hydrate particle in the oil phase: (a) water in the diesel oil dispersed system, (b) most water droplets having been converted into hydrate, and (c) after 10 h of stop mixing.

dx.doi.org/10.1021/ef400147j | Energy Fuels 2013, 27, 2488−2496

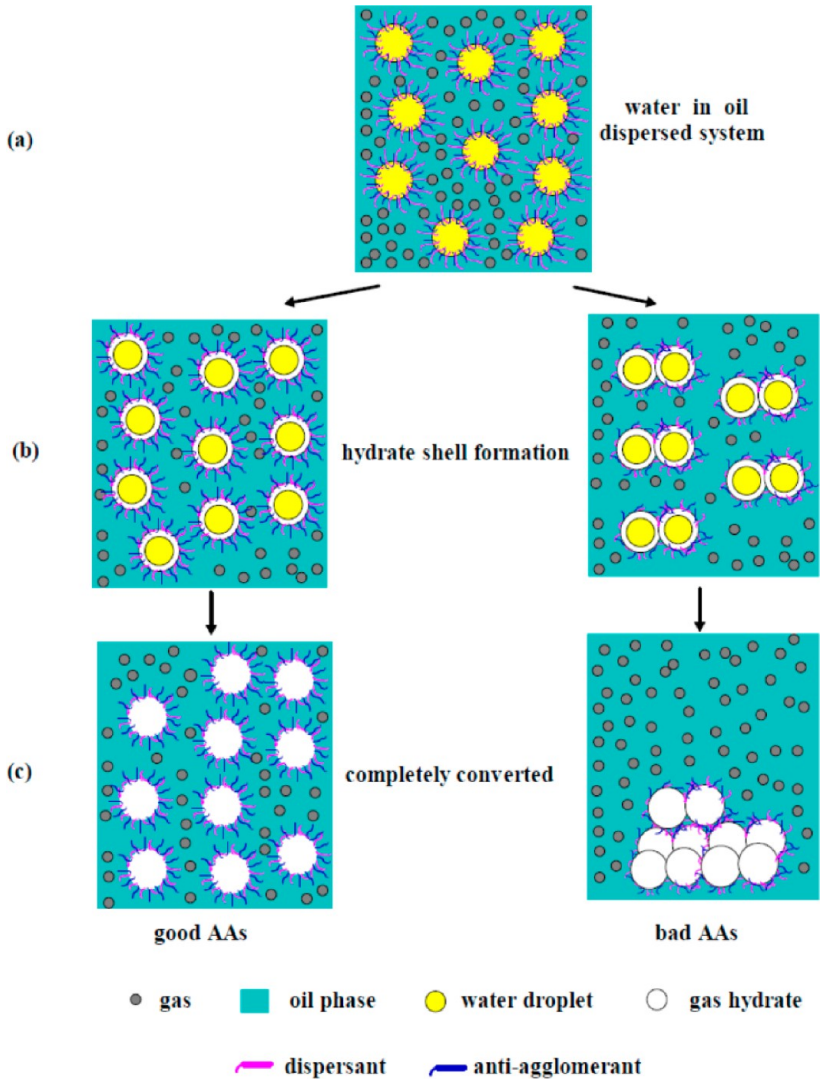

Figure 10. Compounded inhibition mechanisms for AAs.

having been converted into hydrate, and (c) the stirring being shut down for 10 h after the formation of hydrate. From Figure 9, it can be found that the chord length distribution of the water droplet/hydrate particle did not change a lot during these three stages. The median of the chord length distribution of the water droplet/hydrate particle changes from 6.66 μm before methane hydrate formation to 6.10 μm after most of the water droplets converted into hydrate and then to 5.73 μm after 10 h of shutting down the stirrer. The average chord length of the water droplet/hydrate particle is 9.87, 11.11, and 9.78 μm, respectively, at the corresponding three stages. It means that, during the hydrate formation process, only water droplets were transformed into the similar size of the hydrate particle and no agglomeration took place. Hydrate slurry formed from the compounded surfactants also has a high stability and will not result in hydrate agglomeration within as long as 10 h, although the stirring has been shut down.

3.4. Compounded Inhibition Mechanism and Design of New Kind of AA. From the observation and analysis of hydrate formed by adding compounded additives, it can be found that the active mechanism is not similar to those in the literature, which only strengthen the emulsifying effect of AAs. A compounded inhibition mechanism was therefore proposed, as shown in Figure 10. First, water droplets are dispersed in the oil phase evenly, mainly by the effect of one component of the compounded surfactants before gas hydrate formation, as shown in Figure 10a. When hydrate forms the shell shape as described by Taylor et al.[34] and water droplets gradually convert into hydrate, another component of the compounded surfactants begins to play an important role to prevent water droplets with a hydrate shell or hydrate particle from agglomeration, as shown on the left side of panels b and c of Figure 10. With the combined function of the compounded surfactants, the whole water in oil dispersed system can then be translated to the hydrate in oil dispersed system, with the morphology as shown in Figure 8 and well-transported in hydrate slurry form in subsea pipelines. However, if the compounded surfactants do not take action, water droplets surrounded by a hydrate shell or hydrate particle will accumulate into a larger hydrate particle and finally deposit at the bottom of the pipeline, as shown on the right side of panels b and c of Figure 10, with the real morphology as shown in Figure 5c. This process is also in accordance with that described by Turner et al.[29] The profound inhibiting mechanism can be further interpreted by other methods, such as molecular simulation, in the future.

dx.doi.org/10.1021/ef400147j | *Energy Fuels* 2013, 27, 2488−2496

The above evaluations of single and compounded additives have inspired us to synthesize a chemical reagent that may act with good performance of AAs for hydrate. As discussed above, Span 20 may disperse the water droplet into the oil phase evenly, AEO-3 may interact with the hydrate surface to prevent formed hydrate from agglomeration, and alcohols sometimes can be used as co-surfactants. From the structures of Span 20, AEO-3, and alcohols, the main active groups may be alkane ester, ethoxylated, and hydroxyl groups, respectively. According to the compounded inhibition mechanisms and the design by Huo et al.,[15] a new structure of AAs was proposed, as shown in Figure 11. The proposed chemical needs to be further synthesized and tested.

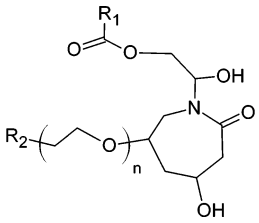

Figure 11. Structure design of a new chemical as a hydrate AA. R1 and R2, long alkanes; *n*, group number.

4. CONCLUSION

Commercial additives were screened to act as hydrate AAs using a sapphire cell and an autoclave with the FBRM probe. Five kinds of hydrate morphologies, clumpy-like, slush-like, flocculent-like, slurry-like, and powder-like, were found during evaluation of the effect of the commercial additives in (water + oil) systems. For a single-additive system, it is usually not suitable to prevent hydrate from agglomerating, although some kinds of single additives can make the formed hydrate as a slurry-like or powder-like morphology. For compounded additive systems with/without the addition of alcohols as co-surfactants, 19 groups of compound additive systems of AEO-3 with other additives were evaluated to examine the performance of anti-agglomeration. The results showed that the compound additive of (2 wt % AEO-3 + 1 wt % Span 20) exhibits good performance of anti-agglomeration. Chord length distribution of the water droplet/hydrate particle in the (5 vol % water + 95 vol % diesel oil) system with the addition of (2 wt % AEO-3 + 1 wt % Span 20) showed that hydrate slurry formed from the compounded surfactants has a high stability and will not result in hydrate agglomeration after more than 10 h, although the stirring has been shut down. A compounded inhibition mechanism, in which one of the components disperses the water droplet in the oil phase and the other component prevents the hydrate formed from agglomerating, was proposed. According to the evaluation of single and compounded additives, a new structure of gas hydrate AA was designed, which needs to be further synthesized and tested.

AUTHOR INFORMATION

Corresponding Author

*Fax: +86-10-89733156. E-mail: cysun@cup.edu.cn (C.-Y.S.); gjchen@cup.edu.cn (G.-J.C.).

Notes

The authors declare no competing financial interest.

ACKNOWLEDGMENTS

The financial support received from the National 973 Project of China (2012CB215004) and the National Natural Science Foundation of China (20925623, U1162205, and 21076225) is gratefully acknowledged.

REFERENCES

(1) Hammerschmidt, E. G. Formation of gas hydrates in natural gas transmission lines. *Ind. Eng. Chem.* **1934**, *26*, 851−855.

(2) Panter, J. L.; Ballard, A. L.; Sum, A. K.; Sloan, E. D.; Koh, C. A. Hydrate plug dissociation via nitrogen purge: Experiments and modeling. *Energy Fuels* **2011**, *25*, 2572−2578.

(3) Fu, B.; Neff, S.; Mathur, A.; Bakeev, K. Novel low dosage hydrate inhibitors for deepwater operations. *Proceedings of the SPE Annual Technical Conference and Exhibition*; New Orleans, LA, Sept 30−Oct 3, 2001; SPE 71472.

(4) Long, Z.; Du, J. W.; Li, D. L.; Liang, D. Q. Phase equilibria of ethane hydrate in $MgCl_2$ aqueous solutions. *J. Chem. Eng. Data* **2010**, *55*, 2938−2941.

(5) Mohammadi, A. H.; Richon, D. Gas hydrate phase equilibrium in the presence of ethylene glycol or methanol aqueous solution. *Ind. Eng. Chem. Res.* **2010**, *49*, 8865−8869.

(6) Li, X. S.; Wu, H. J.; Englezos, P. Prediction of gas hydrate formation conditions in the presence of methanol, glycerol, ethylene glycol, and triethylene glycol with the statistical associating fluid theory equation of state. *Ind. Eng. Chem. Res.* **2006**, *45*, 2131−2137.

(7) Liao, J.; Mei, D. H.; Yang, J. T.; Guo, T. M. Prediction of gas hydrate formation conditions in aqueous solutions containing electrolytes and (electrolytes + methanol). *Ind. Eng. Chem. Res.* **1999**, *38*, 1700−1705.

(8) Kelland, M. A.; Svartaas, T. M.; Dybvik, L. A. Control of hydrate formation by surfactants and polymers. *Proceedings of the SPE International Symposium*; New Orleans, LA, Sept 25−28, 1994; SPE 28506.

(9) Kelland, M. A. History of the development of low dosage hydrate inhibitors. *Energy Fuels* **2006**, *20*, 825−847.

(10) Arjmandi, M.; Tohidi, B.; Danesh, A.; Todd, A. C. Is subcooling the right driving force for testing low-dosage hydrate inhibitors? *Chem. Eng. Sci.* **2005**, *60*, 1313−1321.

(11) Thieu, V.; Frostman, L. M.; Petrolite, B. Use of low-dosage hydrate inhibitors in sour systems. *Proceedings of the 2005 SPE International Symposium on Oilfield Chemistry*; Houston, TX, Feb 2−4, 2005; SPE 93450.

(12) Wang, X. L.; Chen, G. J.; Yang, L. Y.; Zhang, L. W. Study on the recovery of hydrogen from refinery (hydrogen + methane) gas mixtures using hydrate technology. *Sci. China, Ser. B: Chem.* **2008**, *51*, 171−178.

(13) Kelland, M. A.; Svartaas, T. M.; Øvsthus, J.; Tomita, T.; Mizuta, K. Studies on some alkylamide surfactant gas hydrate anti-agglomerants. *Chem. Eng. Sci.* **2006**, *61*, 4290−4298.

(14) Kelland, M. A.; Svartaas, T. M.; Øvsthus, J.; Tomita, T.; Chosa, J. Studies on some zwitterionic surfactant gas hydrate anti-agglomerants. *Chem. Eng. Sci.* **2006**, *61*, 4048−4059.

(15) Huo, Z.; Freer, E.; Lamar, M.; Sannigrahi, B.; Knauss, D. M.; Sloan, E. D. Hydrate plug prevention by anti-agglomeration. *Chem. Eng. Sci.* **2001**, *56*, 4979−4991.

(16) Fotland, P.; Askvik, K. M.; Slamova, E.; Høiland, S.; Borgund, A. E. Natural anti-agglomerants in crude oil: isolation, identification and verification of inhibiting effect. *Proceedings of the 7th International Conference on Gas Hydrates (ICGH 2011)*; Edinburgh, Scotland, U.K., July 17−21, 2011.

(17) Garza, T.; Tsang, Y. H.; Thieu, V.; Stead, P.; Lehmann, M. Development of an improved, non-pitting anti-agglomerant low-dose hydrate inhibitor (AA LDHI) with minimal corrosion potential. *Proceedings of the 7th International Conference on Gas Hydrates (ICGH 2011)*; Edinburgh, Scotland, U.K., July 17−21, 2011.

(18) Pakulski, M.; Qu, Q. Hydrate protection with heat producing three-compinent gas hydrate inhibitor. *Proceedings of the 7th*

International Conference on Gas Hydrates (ICGH 2011); Edinburgh, Scotland, U.K., July 17−21, 2011.
(19) Maccioni, F.; Passucci, C. Torque moment as indicator of low dosage hydrates inhibitors: Effects on multiphase systems. Experimental study on quaternary ammonium and phosphonium compounds. *Proceedings of the 7th International Conference on Gas Hydrates (ICGH 2011)*; Edinburgh, Scotland, U.K., July 17−21, 2011.
(20) Song, W. J.; Xiao, R.; Huang, C.; He, S. H.; Dong, K. J.; Feng, Z. P. Experimental investigation on TBAB clathrate hydrate slurry flows in a horizontal tube: Forced convective heat transfer behaviors. *Int. J. Refrig.* **2009**, *32*, 1801−1807.
(21) Shi, B. H.; Gong, J.; Sun, C. Y.; Zhao, J. K.; Ding, Y.; Chen, G. J. An inward and outward natural gas hydrates growth shell model considering intrinsic kinetics, mass and heat transfer. *Chem. Eng. J.* **2011**, *171*, 1308−1316.
(22) Peng, B. Z.; Chen, J.; Sun, C. Y.; Dandekar, A.; Guo, S. H.; Liu, B.; Mu, L.; Yang, L. Y.; Li, W. Z.; Chen, G. J. Flow characteristics and morphology of hydrate slurry formed from (natural gas + diesel oil/condensate oil + water) system containing anti-agglomerant. *Chem. Eng. Sci.* **2012**, *84*, 333−344.
(23) Chen, L. T.; Sun, C. Y.; Chen, G. J.; Zuo, J. Y.; Ng, H. J. Assessment of hydrate kinetic inhibitors with visual observations. *Fluid Phase Equilib.* **2010**, *298*, 143−149.
(24) Mei, D. H.; Liao, J.; Yang, J. T.; Guo, T. M. Experimental and modeling studies on the hydrate formation of a methane + nitrogen gas mixture in the presence of aqueous electrolyte solutions. *Ind. Eng. Chem. Res.* **1996**, *35*, 4342−4347.
(25) Chen, L. T.; Sun, C. Y.; Nie, Y. Q.; Sun, Z. S.; Yang, L. Y.; Chen, G. J. Hydrate equilibrium conditions of (CH_4 + C_2H_6 + C_3H_8) gas mixtures in sodium dodecyl sulfate aqueous solutions. *J. Chem. Eng. Data* **2009**, *54*, 1500−1503.
(26) Wang, X. L.; Sun, C. Y.; Yang, L. Y.; Ma, Q. L.; Tang, X. L.; Zhao, H. W.; Chen, G. J. Vapor-hydrate equilibria for methane + hydrogen + tetrahydrofuran + water system. *J. Chem. Eng. Data* **2009**, *54*, 310−313.
(27) York, J. D.; Firoozabadi, A. Alcohol cosurfactants in hydrate antiagglomeration. *J. Phys. Chem. B* **2008**, *112*, 10455−10465.
(28) Turner, D. J.; Miller, K. T.; Sloan, E. D. Methane hydrate formation and an inward growing shell model in water-in-oil dispersions. *Chem. Eng. Sci.* **2009**, *64*, 3996−4004.
(29) Turner, D. J.; Miller, K. T.; Sloan, E. D. Direct conversion of water droplets to methane hydrate in crude oil. *Chem. Eng. Sci.* **2009**, *64*, 5066−5072.
(30) Leba, H.; Cameirao, A.; Herri, J. M.; Darbouret, M.; Peytavy, J. L.; Glénat, P. Chord length distributions measurements during crystallization and agglomeration of gas hydrate in a water-in-oil emulsion: Simulation and experimentation. *Chem. Eng. Sci.* **2010**, *65*, 1185−1200.
(31) Redmond, W. *Lasentec D600X Hardware Manual*; Mettler-Toledo Lasentec Product Group, Mettler-Toledo AutoChem, Inc.: Columbia, MD, 2011.
(32) Chen, G. J.; Guo, T. M. A new approach to gas hydrate modelling. *Chem. Eng. J.* **1998**, *71*, 145−151.
(33) Zanota, M. L.; Dicharry, C.; Graciaa, A. Hydrate plug prevention by quaternary ammonium. *Energy Fuels* **2005**, *19*, 584−590.
(34) Taylor, C. J.; Miller, K. T.; Koh, C. A.; Sloan, E. D. Macroscopic investigation of hydrate film growth at the hydrocarbon/water interface. *Chem. Eng. Sci.* **2007**, *62*, 6524−6533.